



# Numerical investigation of a plume from a power generating solar chimney in an atmospheric cross flow

Xinping Zhou<sup>a,b,\*</sup>, Jiakuan Yang<sup>b</sup>, Reccab M. Ochieng<sup>c</sup>, Xiangmei Li<sup>b</sup>, Bo Xiao<sup>b</sup>

<sup>a</sup> Department of Mechanics, School of Civil Engineering and Mechanics, Huazhong University of Science and Technology, 1037 Luoyu Road, Wuhan, Hubei 430074, PR China

<sup>b</sup> Department of Environmental Engineering, School of Environmental Science and Engineering, Huazhong University of Science and Technology, 1037 Luoyu Road, Wuhan, Hubei 430074, PR China

<sup>c</sup> Department of Physics, Maseno University, P.O. Box 333, Maseno, Kenya

## ARTICLE INFO

### Article history:

Received 10 January 2008

Received in revised form 13 April 2008

Accepted 7 May 2008

### Keywords:

Numerical investigation  
Buoyancy-driven plume  
Power generating solar chimney  
Atmospheric cross flow  
Condensation  
Precipitation

## ABSTRACT

A plume in an atmospheric cross flow from a power generating solar chimney is investigated using a three-dimensional numerical simulation model. The simulation model is validated by comparing the data calculated using our model with the numerical simulated results for one-dimensional buoyancy-driven compressible flow in a proposed 1500 m high solar chimney. In this paper, the parametric performances including static pressure, static temperature, density, streamline, and relative humidity field of the flow at the symmetry plane, at the cross plane 2700 m high and at the cross plane 750 m high in the geometry are simulated. It is found that relative humidity of the plume is greatly increased due to the jet of a plume into the surroundings colder than the plume. In addition to a great amount of tiny granules in the plume originating from the ground as effective condensation nuclei of moisture, a condensation would occur, a cloud system and precipitation e.g. rainfall, snow and hail would be formed around the plume when vapor is supersaturated. It is also found that with an increase in chimney height or relative humidity of atmosphere, or a reduction in wind velocity, relative humidity is increased, and increases the probability of precipitation and the potential precipitation areas. Furthermore, the latent heat released from the condensation of supersaturated vapor can aid the plume to keep on rising.

© 2008 Elsevier B.V. All rights reserved.

## 1. Introduction

A solar chimney power generating plant (Schlaich, 1995; Pasurmarthi and Sherif, 1997; Schlaich et al., 2005; Zhou et al., 2007a,b), which consists of three components: an air collector where air is heated, a chimney, and turbine generators situated at the chimney base, is a device where air is driven by buoyancy and drives turbine generators to generate electricity (Fig. 1). A high chimney usually higher than 500 m is needed for large buoyancy and obtaining large capacity of electric power (Schlaich et al., 2005). In recent years, many researchers have undertaken theoretical and numerical investigation of flow through solar chimney

(von Backström and Gannon, 2000; Bonnelle, 2004), solar collector (Bernardes et al., 1999; Zhou et al., 2007b), and turbines (Denantes and Bilgen, 2006; von Backström and Gannon, 2004). However, the plume from a high power generating solar chimney in the atmosphere is rarely referred. The plume's temperature and moisture contents are higher than those of the atmosphere at high heights. Except for Zhou et al. (2008) who simply analyzed the feasibility of a special climate around a commercial solar chimney power plant, no major work exists in this area. Since a floating solar chimney, an innovative concept, proposed by Papageorgiou (2004a,b) which can extend thousands of meters without the technical restrictions or geological limitations encountered by a vertical concrete solar chimney, investigation of the plume with high temperature and high moisture content from a power generating solar chimney in an atmospheric cross flow is more significant for evaluating local atmospheric circulation.

\* Corresponding author. Tel.: +86 27 62773610; fax: +86 27 87792101.

E-mail addresses: [zhxpmark@hotmail.com](mailto:zhxpmark@hotmail.com) (X. Zhou), [yjiakuan@hotmail.com](mailto:yjiakuan@hotmail.com) (J. Yang).

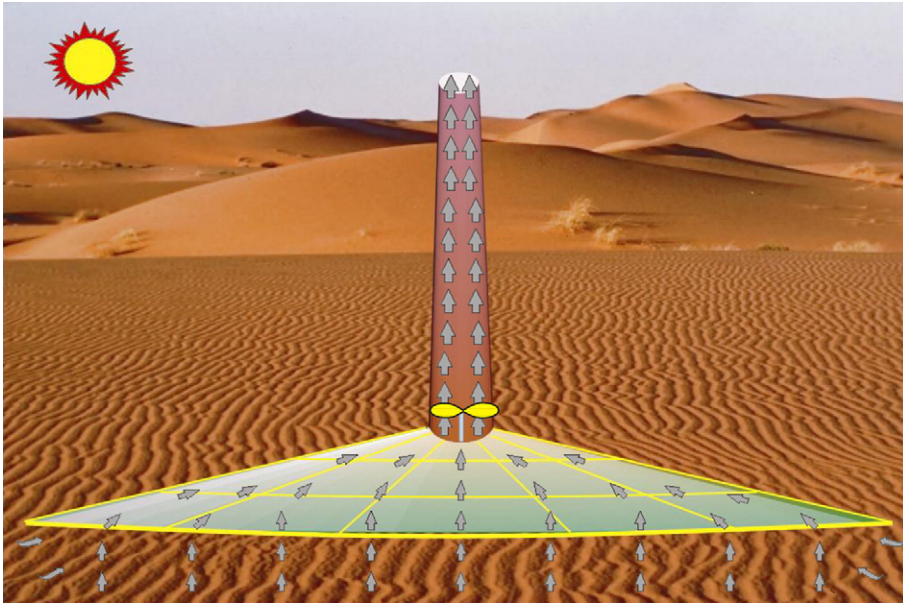


Fig. 1. Schematic diagram of solar chimney power generating system.

Some studies were undertaken to investigate dispersion of a pollutant from a chimney, which is usually far lower than a high power generating solar chimney. Simplified models were used in these studies. Reiquam (1970) used a two-dimensional model to investigate the diffusion of pollutants. Mouzakis and Bergeles (1991) presented a two-dimensional turbulent model to predict the material diffusion of pollutants using a numerical method whereas Mahjoub Saïd et al. (2005) tackled this problem using a three-dimensional turbulent model. König and Mokhtarzadeh-Dehghan (2002) used three-dimensional  $k-\epsilon$  turbulent models to investigate plumes from a multi-flue chimney in the atmosphere.

In this paper, simulation of a plume from a power generating solar chimney in the atmospheric cross flow is carried out in detail using a three-dimensional numerical turbulent model including variation of humidity and condensation of super-saturated vapor.

## 2. Numerical simulation

In order to evaluate the performance of a plume from a power generating solar chimney in an atmospheric cross flow, an exact standard  $k-\epsilon$  turbulent model is developed.

The origin of the Cartesian coordinate system used here is situated at the center of chimney inlet. In the Cartesian coordinate system,  $x$  is in the cross-flow direction,  $y$  is in the span-wise direction, and  $z$  is in the vertical direction.

In the numerical model, air follows the ideal gas law, and only the buoyancy force is considered. The governing equations (Tao, 2001) for conservation of mass, conservation of momentum in  $u$ ,  $v$  and  $w$  directions, conservation of energy, turbulent kinetic energy, and its dissipation rate can be written for the different quantities as follows:

Mass:

$$\frac{\partial}{\partial x_i}(\rho u_i) = S \quad (1)$$

Momentum:

$$\frac{\partial}{\partial x_j}(\rho u_i u_j) = -\frac{\partial p}{\partial x_i} + \frac{\partial \tau_{ij}}{\partial x_j} + S_{u_i} \quad (2)$$

Energy:

$$\frac{\partial}{\partial x_j}(\rho c_p u_j T) = \frac{\partial}{\partial x_j} \left( \lambda \frac{\partial T}{\partial x_j} \right) + \tau_{ij} \frac{\partial u_i}{\partial x_j} + S_T \quad (3)$$

Turbulent kinetic energy:

$$\frac{\partial}{\partial x_j}(\rho u_j k) = \frac{\partial}{\partial x_j} \left( \left( \mu + \frac{\mu_t}{\sigma_k} \right) \frac{\partial k}{\partial x_j} \right) + P_k + G_k - \rho \epsilon \quad (4)$$

Dissipation rate of turbulent kinetic energy:

$$\frac{\partial}{\partial x_j}(\rho u_j \epsilon) = \frac{\partial}{\partial x_j} \left( \left( \mu + \frac{\mu_t}{\sigma_\epsilon} \right) \frac{\partial \epsilon}{\partial x_j} \right) + \frac{\epsilon}{k} (C_1 P_k + C_3 G_k - C_2 \rho \epsilon) \quad (5)$$

where the term produced due to the mean gradients,  $P_k$ , can be given by,

$$P_k = \mu_t \left( \frac{\partial u_i}{\partial x_j} \left( \frac{\partial u_i}{\partial x_j} + \frac{\partial u_j}{\partial x_i} \right) \right), \quad (6)$$

and the term produced due to buoyancy forces,  $G_k$ , can be given by,

$$G_k = -g_i \frac{\mu_t}{\rho \sigma_T} \left( \frac{A \rho}{A x_i} \right). \quad (7)$$

The turbulent viscosity,  $\mu_t$ , can be expressed as,

$$\mu_t = c_\mu \rho k^2 / \epsilon. \quad (8)$$

The constants used in the model have been selected as,

$$c_\mu = 0.09, \quad c_1 = c_3 = 1.44, \quad c_2 = 1.92, \quad \sigma_T = 0.9, \quad \sigma_k = 1.0, \quad \sigma_\epsilon = 1.3, \quad P_r = 0.7,$$

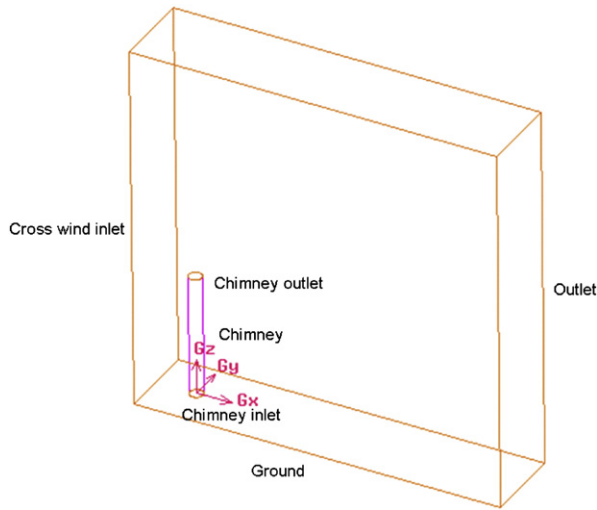


Fig. 2. Model geometry.

The source terms in the equations for conservation of momentum in  $u$ ,  $v$  and  $w$  directions can be expressed in the following forms,

$$S_{u_i} = (\rho - \rho_\infty)g_i. \quad (9)$$

The static pressure of the atmosphere at a height  $h$  is expressed by Zhao (2005) as,

$$p_\infty = p_{\infty 0} \left( 1 - \frac{0.0065h}{T_{\infty 0}} \right)^{5.256} \quad (10)$$

with  $p_{\infty 0}$  being the static pressure at 0 m above sea level.

The static temperature of atmosphere at a height  $h$  is expressed as a function of static temperature at the ground level  $T_{\infty 0}$  and height using the relation

$$T_\infty = T_{\infty 0} - 0.0065h. \quad (11)$$

The cross-wind velocity is distributed as (Xu, 2002),

$$u_\infty = u_{\infty 0} \left( \frac{h}{h_0} \right)^{0.12} \quad (12)$$

with  $u_{\infty 0}$  being the velocity of cross wind at the chimney outlet whose height is  $h_0$ .

Vapor pressure can be expressed as a function of atmospheric pressure and moisture content of air through

$$p_v = p_\infty \frac{d}{0.622 + d}. \quad (13)$$

The saturated vapor pressure has been given by Zhou et al. (1998) as,

$$P_{sv} = P_{sv0} \cdot 10^{8.5(T-273.15)/T} \quad (14)$$

where the saturated vapor pressure at 0 °C,  $P_{sv0}$ , is equal to 608.2 Pa.

**Table 1**  
Boundary conditions

Boundary	Velocity	Temp.	Pressure	Relative humidity	Turbulent energy	Dissipation rate
Chimney outlet	$w = w_0$	$T = T_0$	$P = P_{\infty 0}$	$f = f_0$	$k = 0.005u_0^2$	$\varepsilon = k^{3/2}/0.5/d_c$ (Mahjoub Saïd et al., 2005)
Cross flow	$v = w = 0; u = u_{\infty h}$	$T = T_{\infty h}$	$P = P_{\infty h}$	$f = f_{\infty h}$	$k = 0.005u_{\infty h}^2$	$\varepsilon = k^{3/2}/0.2/H_m$ (Mahjoub Saïd et al., 2005)
Wall including chimney wall		$\frac{\partial T}{\partial n} = 0$				
Ground level		$T = T_{\infty 0}$				

Relative humidity of wet air is defined as,

$$f = \frac{p_v}{p_{sv}}. \quad (15)$$

The density of air which contains vapor can be expressed as,

$$\rho = \frac{p_\infty - p_v}{R_d T} + \frac{p_v}{R_s T} \quad (16)$$

and the atmospheric density can specifically be expressed as,

$$\rho_\infty = \frac{p_\infty - f_\infty p_{sv}}{R_d T} + \frac{f_\infty p_{sv}}{R_s T} \quad (17)$$

with specific gas constant of dry air and specific gas constant of vapor being equal to  $287 \text{ J kg}^{-1} \text{ K}^{-1}$  and  $461 \text{ J kg}^{-1} \text{ K}^{-1}$ , respectively and  $f_\infty$  being the relative humidity of atmosphere.

If  $f < 1$ , vapor is in unsaturated state. The two source terms in the equations for conservation of mass and conservation of energy can be expressed in the following forms,

$$S = 0 \quad (18)$$

and

$$S_T = \rho g_i w \quad (19)$$

where  $w$  is the vertical velocity of air.

If  $f \geq 1$ , we assume that the excess vapor is condensed into liquid water, and that the liquid water condensed is immediately separated from the plume to form cloud or precipitation. The two source terms can be expressed in the following forms,

$$S = \left( \frac{p_v}{R_s T} - \frac{p_{sv}}{R_s T} \right) u_i \quad (20)$$

and

$$S_T = \left( \frac{p_v}{R_s T} - \frac{p_{sv}}{R_s T} \right) L + \rho g_i w \quad (21)$$

where the latent heat released from condensation of vapor,  $L$ , can be given by

$$L = 2,502,535.259 - 212.56384T. \quad (22)$$

The specific heat capacity of wet air,  $c_p$ , is expressed as

$$c_p = 1,010 + 1,880d. \quad (23)$$

The model geometry shown in Fig. 2, is 4500 m long, 4500 m high and 1000 m wide. The center of a 1500 m high chimney is located 580 m downstream of the cross-flow inlet. In this model, the effect of the heat transferred from the top of the collector to the air is neglected.

The numerical code uses the finite volume method. The solutions of equations are based on the algorithm Semi-

**Table 2**

Parametric performances at inlet and outlet of a 1500 m high chimney simulated using our model

Parameter	$P_{ch,in}/$ kPa	$P_{ch,out}/$ kPa	$T_{ch,in}/$ K	$T_{ch,out}/$ K	$\rho_{ch,in}/$ kg m <sup>-3</sup>	$\rho_{ch,out}/$ kg m <sup>-3</sup>	$V_{ch,in}/$ m s <sup>-1</sup>	$V_{ch,out}/$ m s <sup>-1</sup>
Value	101	85	338.2	323.5	1.04	0.91	15.95	18.94

Implicit Method for Pressure-Linked Equations (SIMPLE) proposed by Patankar (1980).

The boundary conditions in the model are summarized in Table 1. The performance including temperature, velocity, and relative humidity of airflow at the chimney outlet is solved for the flow inside the chimney. In the model, static pressure difference has an influence on the plume in terms of buoyancy. In order to clear up the repeated influence of static pressure difference of air between low height and high heights on the plume in atmospheric cross flow inside the geometry, the static pressures at the chimney outlet and the cross-flow inlet and outlet are all defined as the value of atmospheric static pressure at the ground level.

The iterative process in the computation is stopped when the convergence criterion defined as

$$\left| \frac{f^{m+1} - f^m}{f^{m+1}} \right| \leq \delta_i \quad (24)$$

is satisfied. In Eq. (24),  $f$  stands for continuity, velocity components, energy,  $k$  and  $\epsilon$ ,  $m$  is the iteration number while  $\delta_i$  are the convergence criteria. Conservation of mass has been checked and the stability of the values has been checked in order to make the values have nearly no variation.

### 3. Validation

Validation of the numerical model for a buoyancy-driven compressible flow which rises by many meters is done in this work by comparing the data calculated using our model with the numerical simulated results for one-dimensional buoyancy-driven compressible flow in a proposed 1500 m high solar chimney with an inner diameter of 160 m (von Backström and Gannon, 2000) at a site where the typical atmospheric conditions are 298.2 K and 101 kPa. The rise in temperature of air at the collector outlet, which is determined by collector area,

**Table 3**

Comparison of performance simulated using our model and numerical simulated results for one-dimensional buoyancy-driven compressible flow in a proposed 1500 m high solar chimney (von Backström and Gannon, 2000)

Parametric ratio	Static pressure ratio	Total temp. laps/K	Density ratio	Velocity ratio
Calculated results using our model	0.84	0.0432	0.873	1.187
Numerical simulated results for one-dimensional buoyancy-driven compressible flow	0.856	0.0433	0.895	1.142
Difference of numerical simulated results for one-dimensional buoyancy-driven compressible flow/%	1.87	0.23	2.46	3.94

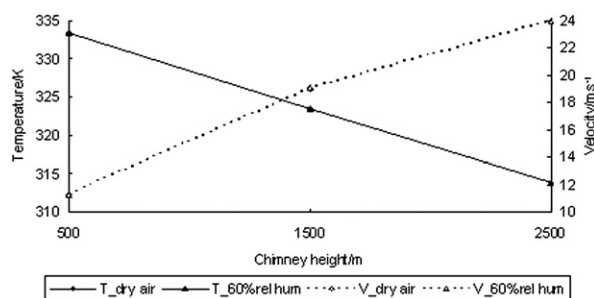


**Fig. 3.** Variations of temperature and velocity of outflow of chimneys with different heights for dry air and wet air with relative humidity of 60%.

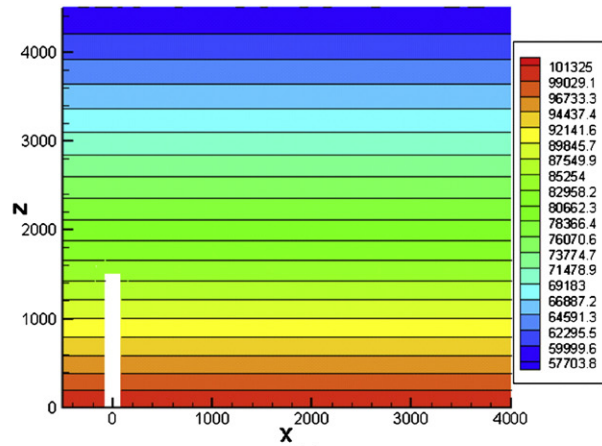
turbine efficiency, etc., can reach 20–60 K when the efficiency of on-load turbines is equal to 80% (Mullet, 1987). In this validation, the rise in temperature is taken to be 40 K at which dry air works as a fluid. The boundary conditions are summarized as follows: all the velocity components in three directions is equal to 0; total pressure at the chimney inlet is defined as atmospheric static pressure at the ground level since that total pressure at the chimney inlet is equal to the sum of static pressure and dynamic pressure at the collector inlet where the dynamic pressure is negligible compared with static pressure. Static pressure at the chimney outlet is defined as atmospheric static pressure at the ground level in order to clear up repeated influence of static pressure difference of the air between the collector inlet and the chimney outlet level to the flow (Zhou et al., in press). The boundary conditions are similar to those in the model since both the flows are buoyancy-driven compressible flows.

In the simulation of buoyant flow through a solar chimney, the factor of pressure drop at the turbines which is used in transferring the kinetic energy of the turbine is considered. Schlaich (1995) and Schlaich et al. (2005) in succession recommended the lower values of 2/3 and 0.8. In other works, Bernardes et al. (2003) mentioned a high value of 0.97. von Backström and Fluri (2006) reported the expression  $\frac{n-m}{n+1}$ , which is typically between 2/3 and 1, where  $m$  is the pressure potential exponent, which is typically a negative number between -1 and 0, and  $n$  is the pressure loss exponent which is typically 2. In order to make convenient calculations, a value of 0.9 is used in this simulation.

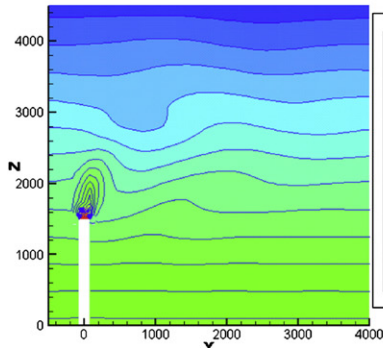
The parametric performances at the inlet and the outlet simulated using our model is presented in Table 2. With an increase in height from the inlet to the outlet, the pressure is normally reduced, and the temperature is gradually reduced due to energy conversion to gravitational potential energy (von Backström and Gannon, 2000). With an increase in height, the pressure lapses faster than the temperature, which results in the decrease in density from the inlet to outlet according to the state equation. Finally, the decrease in density induces the increase in velocity as required by conservation of mass.

Table 3 presents the comparison of the ratios of parametric performances including static pressure, total temperature, density and velocity at the outlet to those at the inlet using our model with the numerical simulated results for one-dimensional buoyancy-driven compressible flow in a proposed 1500 m high solar chimney.

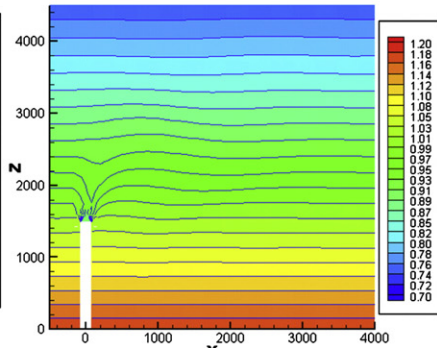
As shown in Table 3, agreements within a difference of 4% for the ratios are obtained. The gaps which exist arise due to the fact that the model adopted is standard  $k-\epsilon$  turbulent model, which



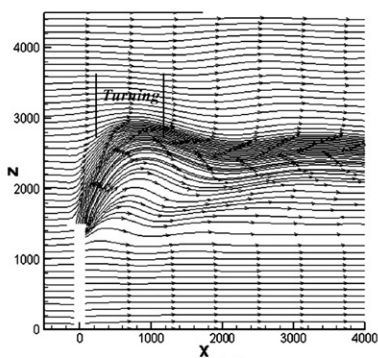
(a)



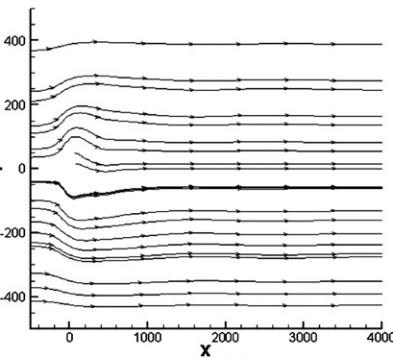
(b)



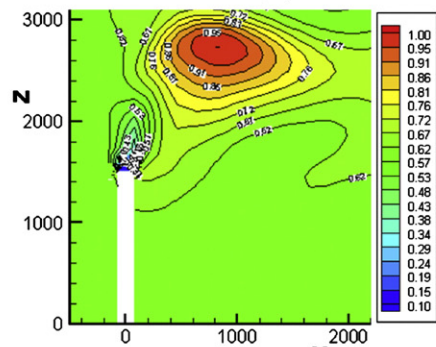
(c)



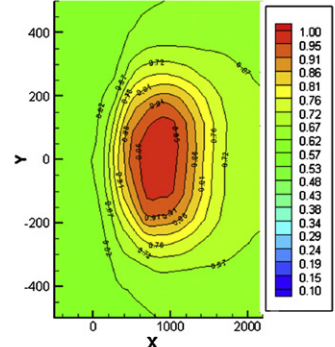
(d)



(e)



(f)



(g)

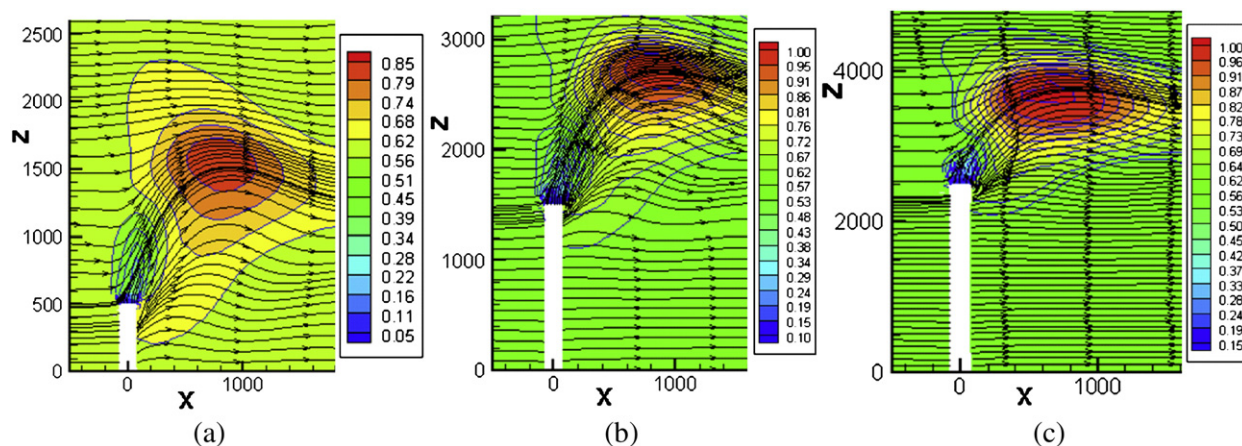


Fig. 5. Streamlines and relative humidity field at symmetry plane for chimneys with different heights: (a) 500 m; (b) 1500 m; (c) 2500 m.

is different from the von Backström and Gannon's model using one-dimensional inviscid model. This strongly supports the idea that the numerical model is exact for buoyancy-driven flow.

## 4. Results and discussions

### 4.1. Typical parametric performances

This work is based on a theoretical 1500 m high power generating solar chimney with an inner diameter of 160 m at a site where the typical atmospheric conditions are about 298.2 K and 101 kPa (von Backström and Gannon, 2000). The rise in temperature of air at the collector outlet where turbines are on load is assumed to be 40 K. The initial parameters of atmospheric cross flow are summarized as follows: relative humidity of atmosphere is 60%, and wind velocity at the chimney outlet level is  $5 \text{ m s}^{-1}$ . It is assumed in this work that when relative humidity is more than 100%, the excessive vapor condenses into liquid water with its latent heat used in heating the flow. Furthermore, much more tiny granules exist in the atmosphere at the ground level. These tiny granules taken from the ground to the high height together with air by convection can be used as effective condensation nuclei of moisture. Therefore, condensation would occur and a cloud system would be formed, and even a precipitation would be formed around the plume.

Fig. 3 presents the variations of temperature and velocity of the outflow of chimneys with different heights for dry air and wet air with 60% of relative humidity. As shown in Fig. 3, with an increase in chimney height, temperature of the outflow decreases due to more thermal energy being converted to gravitational potential energy. This results in the reduction in density induced by the reduction in pressure and the increase in velocity. However, the difference of the performances of the chimney outflows for different humidity of air is negligible as shown in Fig. 3. For example, the velocities for dry air and wet air with 60% of relative humidity released from the chimney outlet are respectively  $18.94 \text{ m s}^{-1}$  and  $19.07 \text{ m s}^{-1}$ . It is a fact that the chimney inward air density

and atmospheric density synchronously decrease with an increase of relative humidity of atmosphere and will lead to insignificant variation of buoyancy according to Eqs. (16) and (17). It is found that the performance of the chimney outflow is not nearly influenced by atmospheric humidity for any chimney height.

Fig. 4 shows the typical parametric performances including static pressure, static temperature, density, streamline, and relative humidity field of plume in an atmospheric cross flow at the symmetry plane, at the cross plane 2700 m high and at the cross plane 750 m high in the geometry.

Fig. 4a presents the pressure field at the symmetry plane in the geometry. In the figure, the pressure is reduced from 101 kPa to 58 kPa with an increase in height from the ground to the 4500 m height.

Fig. 4b shows the temperature field at the symmetry plane in the geometry. In the figure, the atmospheric temperature is reduced from 298.2 K at the ground level to 268.9 K at the 4500 m height, and bulges emerge on the temperature profiles over the chimney since the chimney outflow is warmer than the surroundings. Depressions also emerge on the temperature profiles around the turnings.

Fig. 4c shows the density field at the symmetry plane in the geometry. In the figure, the atmospheric density is reduced from  $1.18 \text{ kg m}^{-3}$  at the ground level to  $0.75 \text{ kg m}^{-3}$  at the 4500 m height, and depressions emerge on the density profiles over the chimney. This depends on smaller density of the plume than the surroundings is determined by higher temperature as shown in Fig. 4b.

It is known the temperature of plume lapses faster than the atmosphere due to heat diffusion between the plume and the atmosphere by convection and energy conversion to gravitational potential energy.

Fig. 4d presents the streamlines of plume in atmospheric cross flow at the symmetry plane in the geometry. In the combination of initial momentum and buoyancy-driven force, the flow rises with its temperature reduced. When its temperature is reduced in rising to a value of the atmospheric temperature at the same height, the plume with a velocity

Fig. 4. Typical parametric performances at symmetry plane, at 2700 m high cross plane and at 750 m high cross plane: (a) Static pressure field at symmetry plane; (b) Static temperature field at symmetry plane; (c) Density field at symmetry plane; (d) Streamline at symmetry plane; (e) Streamline at 750 m high cross plane; (f) Relative humidity field at symmetry plane; (g) Relative humidity field at 2700 m high cross plane.

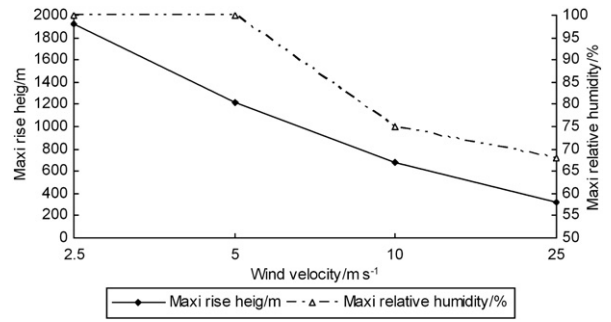
**Table 4**  
Rise in height of plume released from chimneys with different chimney heights

Chimney height/m	Initial velocity/m s <sup>-1</sup>	Temp. difference/K	Maximum height/m	Rise in height/m
500	11.30	38.4	1500	1000
1500	19.07	35.1	2720	1220
2500	24.04	31.9	3750	1250

goes on rising with its temperature continuously reducing to lower value than the surroundings as shown in Fig. 4b, and reaches a maximum height of about 2720 m at about 850 m away from the center of the chimney in the cross-flow direction where vertical component of airflow velocity is equal to 0. After rising to the maximum height, the plume starts to descend by negative buoyancy because its temperature is lower than the surroundings and finally the plume keeps parallel with the ground.

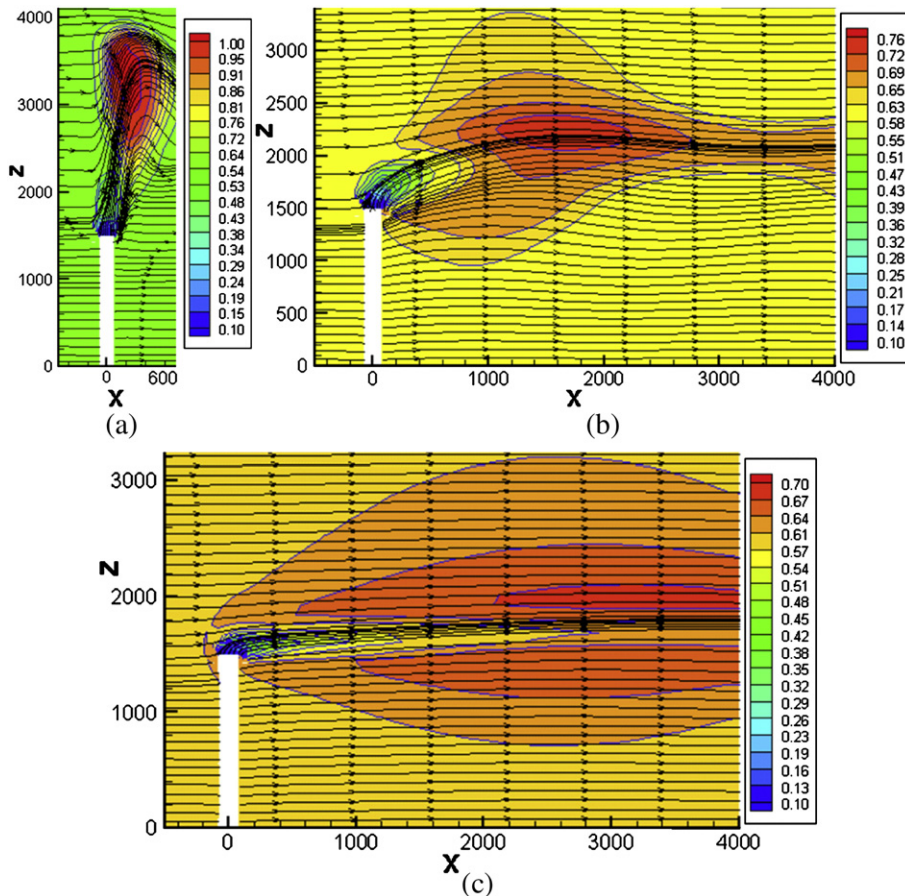
Fig. 4e presents the streamline of flow at the 750 m high cross plane in the geometry.

Fig. 4f presents the relative humidity field at the symmetry plane and Fig. 4g shows the relative humidity field at the 2700 m high cross plane in the geometry. As shown in Fig. 4f and g, the relative humidity reaches 12.5% at the chimney outlet, and increases with rising plume and



**Fig. 7.** Variations of maximum rise in height and maximum relative humidity with wind velocity.

reaches maximum values around the turnings. At the 2740 m height vapor is supersaturated, and then condensation occurs with latent heat used to heat the plume. With an increase in height, saturated vapor pressure lapses faster than atmospheric static pressure, inducing the reduction in moisture content to satisfy the assumption of the same relative humidity according to Eqs. (13) and (14). This distribution of moisture content is in accordance with the normal distribution of moisture content in the atmosphere (Zhou et al., 1998). In other words, the vapor content in the plume originating



**Fig. 6.** Streamlines and relative humidity field at symmetry plane subjected to different wind velocities: (a) 2.5 m s<sup>-1</sup>; (b) 10 m s<sup>-1</sup>; (c) 25 m s<sup>-1</sup>.

from the ground is more than that in high atmosphere with the same relative humidity. When a plume is ejected into atmospheric cross flow at high heights, vapor content in air around the chimney outlet will be greatly increased.

We also found that the relative humidity in an area which is far larger than the plume area is obviously higher than far side atmosphere at the same heights as shown in Fig. 4f and g. For example, the area where relative humidity is higher than 95% is between 2500 m and 2850 m in the vertical direction, between 640 m and 1060 m in the cross-flow direction, and between -120 m and 120 m in the span-wise direction. The significant increase in humidity of atmosphere is induced by material diffusion of the plume including inward vapor.

#### 4.2. Variations with chimney height

Fig. 5 shows streamlines and relative humidity field of the plume in an atmospheric cross flow with different chimney heights of 500 m and 2500 m. All the ambient relative humidity of atmospheric air is kept constant at a value of 60%.

Combination of initial jet and the buoyancy-driven force results in the rising of plume in atmospheric cross flow. Rise in height is proportional to initial velocity and temperature difference of the plume and the ambient (Guo and Ruan, 2001). Table 4 gives the rise in height of the plume released from chimneys with different chimney heights. As shown in Fig. 3 and Table 4, the performances of outflow have a correlation with chimney heights. As the chimney height increases from 500 m to 1500 m to 2500 m, initial velocity also increases while the temperature difference decreases. This results in no significant difference as the rises in height from 1000 m to 1220 m to 1250 m for the three given chimney heights from 500 m to 1500 m to 2500 m.

As shown in Fig. 5, the maximum relative humidity increases with height of the chimney which is usually at the turnings of the plume, and the volume of liquid water condensed is highest for the 2500 m tall chimney. The temperature of plume from a higher chimney in the upper atmosphere is lower, resulting in smaller saturated vapor pressure resulting in larger relative humidity as given by Eq. (14).

In order to produce electric power economically, the radius of the collector in commercial solar chimney power plants usually is several kilometers (Schlaich et al., 2005). Accordingly, the potential precipitation areas being within 1000 m in the cross-flow direction are just over the collector.

#### 4.3. Variations with wind velocity

We present the evolution of a plume from a chimney and visualization of relative humidity field subjected to different wind velocity at the chimney outlet levels of  $2.5 \text{ m s}^{-1}$ ,  $5 \text{ m s}^{-1}$ ,  $10 \text{ m s}^{-1}$  and  $25 \text{ m s}^{-1}$  in Figs. 5b and 6. The figures show that atmospheric cross flow affects the flows of the plumes. When the wind velocity is low, the plume dominates the flow, inducing significant rising of the plume and then more relative humidity as shown in Fig. 7. It may also be noticed that with an increase in wind velocity, the turnings of the plume are smoother, for example, the turnings for  $25 \text{ m s}^{-1}$  wind velocity never emerge because the atmospheric wind dominates the flow. Also, the potential precipitation area for larger wind velocity is more adjacent to the chimney, for example, the potential precipitation area for  $2.5 \text{ m s}^{-1}$  wind velocity is just within 400 m away from the chimney center in the cross-flow direction, while that for  $5 \text{ m s}^{-1}$  wind velocity is within 900 m.

#### 4.4. Variations with relative humidity

Fig. 8 shows the variations of streamlines and relative humidity field of the flow in an atmospheric cross flow with different relative humidity of 40% and 80%. As shown in Figs. 5b and 8, the probability of precipitation and the potential precipitation areas increase with relative humidity of atmosphere.

#### 4.5. Effect of latent heat

Fig. 9 gives comparison of streamlines and relative humidity field of the flow with and without the latent heat released from condensation of supersaturated vapor used to heat the plume based on atmospheric relative humidity of

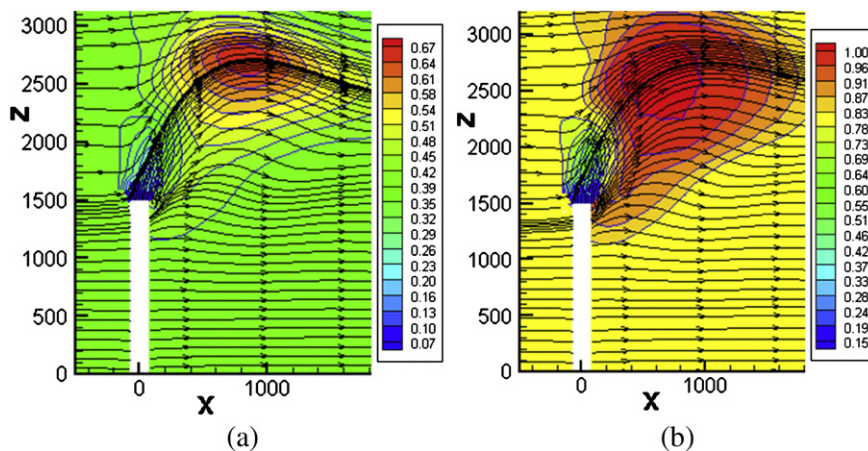
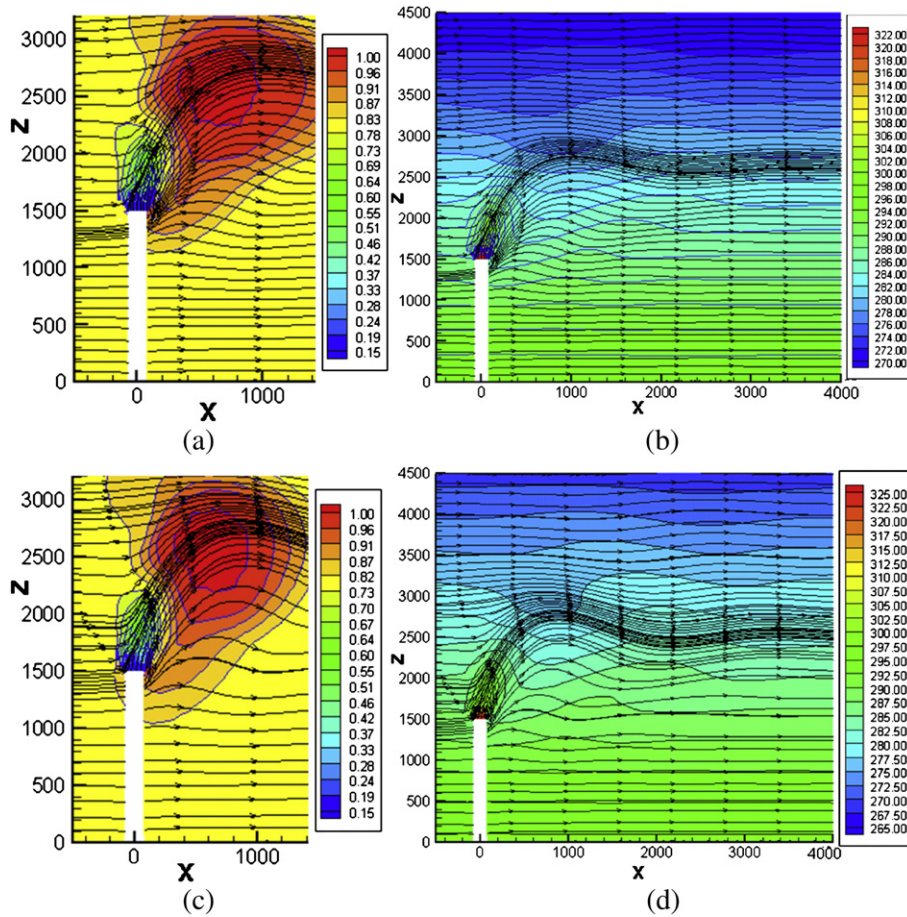


Fig. 8. Streamlines and relative humidity field at symmetry plane for atmospheric cross flow with relative humidity: (a) 40%; (b) 80%.



**Fig. 9.** Comparisons of temperature field, streamlines and relative humidity field of flow with and without latent heat released from condensation of supersaturated vapor: (a) Streamline and relative humidity field at symmetry plane with latent heat; (b) Streamline and temperature field at symmetry plane with latent heat; (c) Streamline and relative humidity field at symmetry plane without latent heat; (d) Streamline and temperature field at symmetry plane without latent heat.

80%. In the figures, the maximum height for the case without the latent heat is 2700 m, which is lower than that with the latent heat which is 2720 m. It is also found that the depressions of temperature profiles around the turnings for the case without the latent heat are drastic for latent heat released from the condensation of supersaturated air. The phenomena show that the latent heat released from condensation of supersaturated vapor which is used to heat the plume helps the plume to keep on rising.

## 5. Conclusions

A numerical simulation of a plume from a power generating solar chimney in an atmospheric cross flow was performed in this paper. Conclusions drawn from the analyses are:

- 1) Parametric performances including static pressure, static temperature, density, streamline, and relative humidity field of flow at the symmetry plane, at the cross plane 2700 m high and at the cross plane 750 m high in the geometry when simulated showed that relative humidity was greatly increased due to jet of a plume originating from the ground level. Furthermore, a great amount of tiny

granules from the ground is taken by the plume to high level as effective condensation nuclei of moisture. When vapor was supersaturated, a condensation of the excessive vapor to liquid water would occur, and then a cloud system and even precipitation would be formed around the plume.

- 2) Sensitivity analyses of parametric performances of the flow were performed by changing the parameters including chimney height, relative humidity of atmosphere, and wind velocity in the simulation and it was found that with an increase in chimney height or relative humidity of atmosphere, or a reduction in wind velocity, relative humidity is increased. There was also an increase in the probability of precipitation and the potential precipitation areas.
- 3) The effect of latent heat from condensation of supersaturated vapor on the performances of the plume was analyzed with results showing that the latent heat could aid the plume to keep on rising.

## Acknowledgements

This research is supported by the outstanding doctorate thesis Foundation of Huazhong University of Science and

Technology, the Youth Chenguang Project of Science and Technology of Wuhan City of China under two Grants No. 20015005037 and No. 20055003059-34 and the Natural Science Foundation of Hubei Province under Grant No. 2005ABA047.

## References

- Bernardes, M.A. dos S., Valle, R.M., Cortez, M.F., 1999. Numerical analysis of natural laminar convection in a radial solar heater. *International Journal of Thermal Sciences* 38, 42–50.
- Bernardes, M.A. dos S., Vob, A., Weinrebe, G., 2003. Thermal and technical analyzes of solar chimneys. *Solar Energy* 75, 511–524.
- Bonnelle, D., Solar Chimney, water spraying Energy Tower, and linked renewable energy conversion devices: presentation, criticism and proposals, Doctoral thesis, University Claude Bernard-Lyon 1, France; July, 2004. Registration Number: 129–2004.
- Denantes, F., Bilgen, E., 2006. Counter-rotating turbines for solar chimney power plants. *Renewable Energy* 31, 1873–1891.
- Guo, J., Ruan, Y.L., 2001. *Air Pollution Control Engineering*. Chemical Industry Press, Beijing, China.
- König, C.S., Mokhtarzadeh-Dehghan, M.R., 2002. Numerical study of buoyant plumes from a multi-flue chimney released into an atmospheric boundary layer. *Atmospheric Environment* 36, 3951–3962.
- Mahjoub Saïd, N., Mhiri, H., Palec, G.L., Bourno, P., 2005. Experimental and numerical analysis of pollutant dispersion from a chimney. *Atmospheric Environment* 39, 1727–1738.
- Mouzakis, F.N., Bergeles, G., 1991. Pollutant dispersion over a triangular ridge: a numerical study. *Atmospheric Environment* 25A (12), 371–379.
- Mullet, L.B., 1987. The solar chimney overall efficiency, design and performance. *International Journal of Ambient Energy* 8 (1), 35–40.
- Papageorgiou, C.D., 2004a. Floating Solar Chimney Technology. . accessed at: <http://www.floatingsolarchimney.gr>.
- Papageorgiou, C.D., 2004b. Optimum design for solar power stations with floating solar chimneys. *Proceeding of ISES Asia Pacific Solar Energy Conf.*, Kwangju, Korea, pp. 763–772.
- Pasurmarthi, N., Sherif, S.A., 1997. Performance of a demonstration solar chimney model for power generation. *Proceeding of the 1997 35th Heat Transfer and Fluid, Sacramento*, pp. 203–240.
- Patankar, S.V., 1980. *Numerical heat transfer and fluid flow*. McGraw-Hill, New York.
- Reiquam, H., 1970. An atmospheric transport and accumulation model for airsheds. *Atmospheric Environment* 4, 233–247.
- Schlaich, J., 1995. *The Solar Chimney: Electricity from the Sun*, Geislingen, Germany.
- Schlaich, J., Bergermann, R., Schiel, W., Weinrebe, G., 2005. Design of commercial solar updraft tower systems—utilization of solar induced convective flows for power generation. *Journal of Solar Energy Engineering* 127, 117–124.
- Tao, W.Q., 2001. *Numerical Heat Transfer*, 2nd edn. Jiaotong University Press, Xi'an, China.
- von Backström, T.W., Gannon, A.J., 2000. Compressible flow through solar power plant chimneys. *Journal of Solar Energy Engineering* 122, 138–145.
- von Backström, T.W., Gannon, A.J., 2004. Solar chimney turbine characteristics. *Solar Energy* 76, 235–241.
- von Backström, T.W., Fluri, T.P., 2006. Maximum fluid power condition in solar chimney power plants—an analytical approach. *Solar Energy* 80, 1417–1423.
- Xu, Z.J., 2002. *Design and calculation of the foundation of tower*. China Petrochemical Press, Beijing, China.
- Zhao, H.Z., 2005. *Engineering fluid mechanics*. Huazhong University of Science and Technology Press, Wuhan, China.
- Zhou, S.Z., Zhang, R.Y., Zhang, C., 1998. *Meteorology and climatology*, 3rd edn. Higher Education Press, Beijing, China.
- Zhou, X.P., Yang, J.K., Xiao, B., Hou, G.X., 2007a. Simulation of a pilot solar chimney power equipment. *Renewable Energy* 32, 1637–1644.
- Zhou, X.P., Yang, J.K., Xiao, B., Hou, G.X., 2007b. Experimental study of temperature field in a solar chimney power setup. *Applied Thermal Engineering* 27, 2044–2050.
- Zhou, X.P., Yang, J.K., Xiao, B., Shi, X.Y., 2008. Special Climate Around a Commercial Solar Chimney Power Plant. *J. Energy Engineering, ASCE* 134, 6–14.
- Zhou, X.P., Yang, J.K., Wang, J.B., Xiao, B., Hou, G.X., Wu, Y.Y., in press Numerical investigation of a flow through solar chimney. *Heat Transfer Engineering*.